Science Signaling
AAAS

www.sciencesignaling.org/cgi/content/full/2/58/ra6/DC1

Supplementary Materials for

The Precise Sequence of FGF Receptor Autophosphorylation Is Kinetically Driven and Is Disrupted by Oncogenic Mutations

Erin D. Lew, Cristina M. Furdui, Karen S. Anderson, Joseph Schlessinger*

*To whom correspondence should be addressed. E-mail: joseph.schlessinger@yale.edu

Published 17 February 2009, *Sci. Signal.* **2**, ra6 (2009)
DOI: 10.1126/scisignal.2000021

This PDF file includes:

Supplementary Materials

Figure S1. Identification of Tyrosine Phosphorylation Sites on Kinase-Dead Mutants with ESI-MS and MS/MS. Each of the kinase-dead samples analyzed by native-PAGE was subjected to in gel trypsin digestion. The resulting tryptic digest for each phosphorylation state was further analyzed by nano-LC (Dionex Ultimate3000 System) coupled to a Thermo ESI LTQ mass spectrometer. A typical gradient was run for 60 min from 0 to 100% solvent B (80% acetonitrile, 20% H_2O and 0.1% formic acid). Solvent A consisted of 5% acetonitrile, 95% H_2O and 0.1% formic acid. The flow rate was set at 200 nL/min on a 75 µm x 10 cm fused silica capillary column (New Objectives) in-house packed with Michrom Magic C18AQ (200 Å, 5 µm). The ESI LTQ mass spectrometer was operated in selected ion monitoring mode (SIM) for precursor ions corresponding to the peptides containing unphosphorylated and phosphorylated tyrosine residues. The peptide identification was performed automatically using the Bioworks 3.1 software. The generated peptide list was ranked by XCorr to charge state ratio and the phosphorylation sites were identified for each phosphorylation state. Representative MS/MS spectra for the phosphorylated **(A)** Y^{583}KD and **(B)** Y^{654}KD are shown.

Figure S1

A.

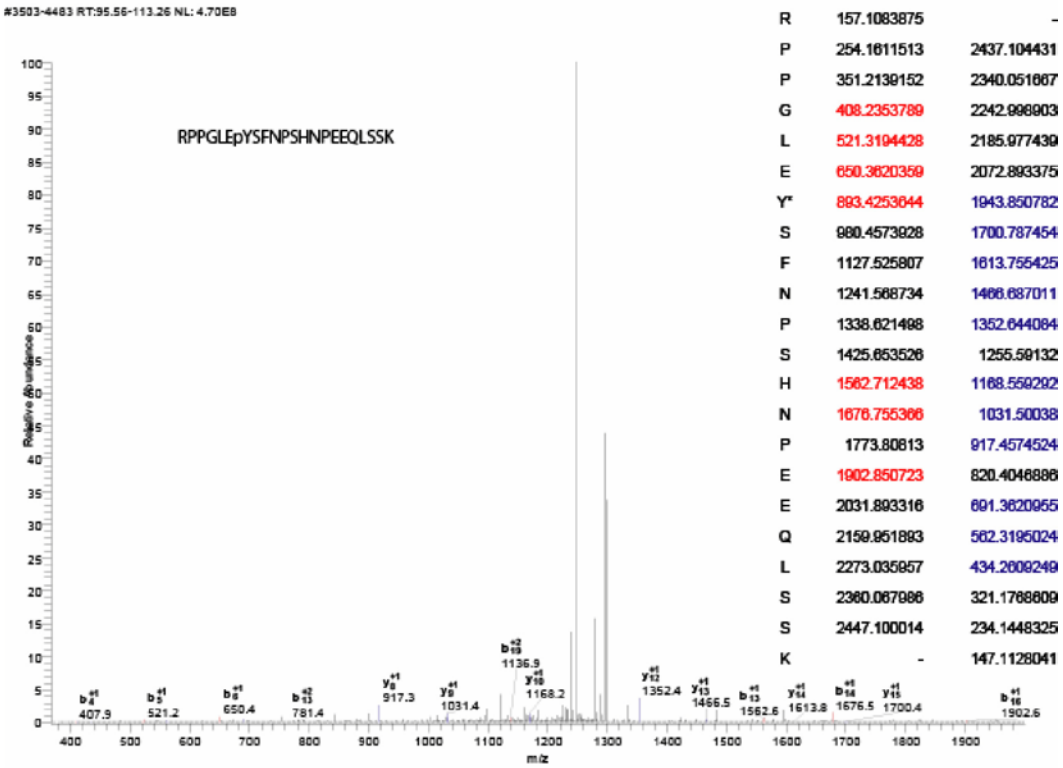

AA	b ions	y ions
R	157.1083875	-
P	254.1611513	2437.104431
P	351.2139152	2340.051667
G	408.2353789	2242.996903
L	521.3194428	2185.977439
E	650.3620359	2072.893375
Y*	893.4253644	1943.850782
S	980.4573928	1700.787454
F	1127.525807	1613.755425
N	1241.568734	1466.687011
P	1338.621498	1352.644084
S	1425.653526	1255.59132
H	1562.712438	1168.559292
N	1676.755366	1031.50038
P	1773.80813	917.4574524
E	1902.850723	820.4046886
E	2031.893316	691.3620955
Q	2159.951893	562.3195024
L	2273.035857	434.2609249
S	2360.067986	321.1768609
S	2447.100014	234.1448325
K	-	147.1128041

B.

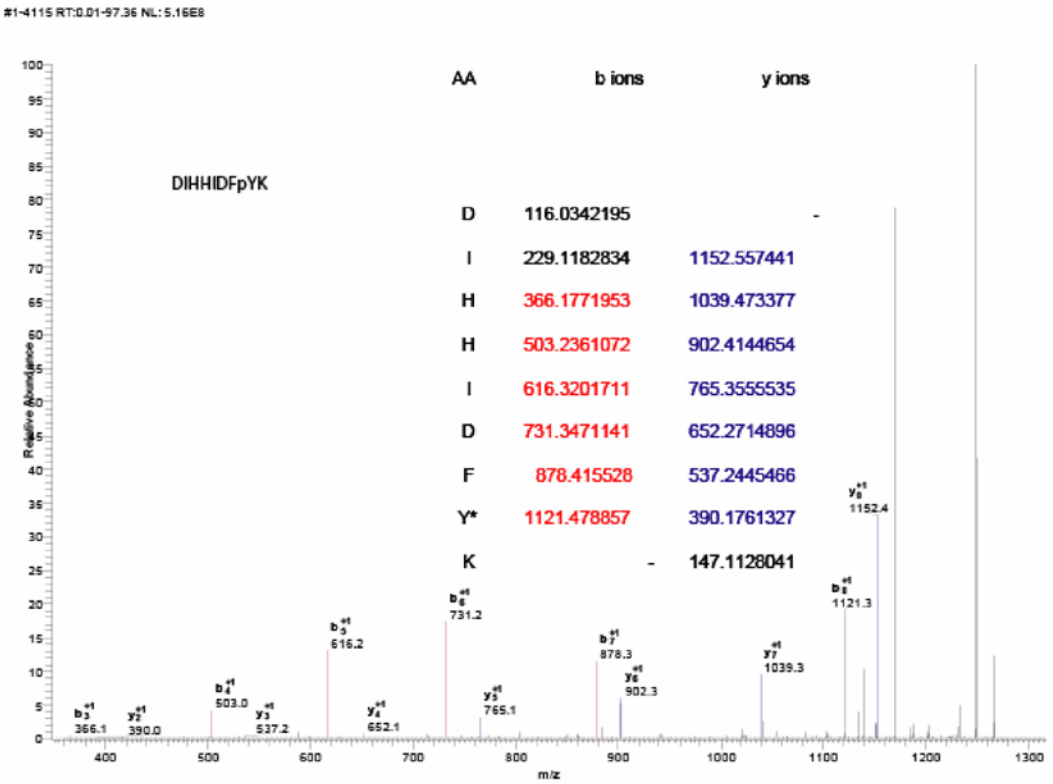

AA	b ions	y ions
D	116.0342195	-
I	229.1182834	1152.557441
H	366.1771953	1039.473377
H	503.2361072	902.4144654
I	616.3201711	765.3555535
D	731.3471141	652.2714896
F	878.415528	537.2445466
Y*	1121.478857	390.1761327
K	-	147.1128041

Figure S2. Identification of Tyrosine Phosphorylation Sites of N546K Glioblastoma using ESI-MS and MS/MS. The N546K mutant was analyzed by native-PAGE was subjected to in gel trypsin digestion. The resulting tryptic digest for each phosphorylation state was further analyzed by nano-LC (Dionex Ultimate3000 System) coupled to a Thermo ESI LTQ mass spectrometer. A typical gradient was run for 60 min from 0 to 100% solvent B (80% acetonitrile, 20% H_2O and 0.1% formic acid). Solvent A consisted of 5% acetonitrile, 95% H_2O, and 0.1% formic acid. The flow rate was set at 200 nL/min on a 75 µm x 10 cm fused silica capillary column (New Objectives) in-house packed with Michrom Magic C18AQ (200 Å, 5 µm). The ESI LTQ mass spectrometer was operated in selected ion monitoring mode (SIM) for precursor ions corresponding to the peptides containing unphosphorylated and phosphorylated tyrosine residues. The peptide identification was performed automatically using the Bioworks 3.1 software. The generated peptide list was ranked by XCorr to charge state ratio and the phosphorylation sites were identified for each phosphorylation state. Representative MS/MS spectra for the unphosphorylated tyrosine containing peptides for N546K glioblastoma mutant to determine the order of autophosphorylation are shown in **(A-B).**

Figure S2

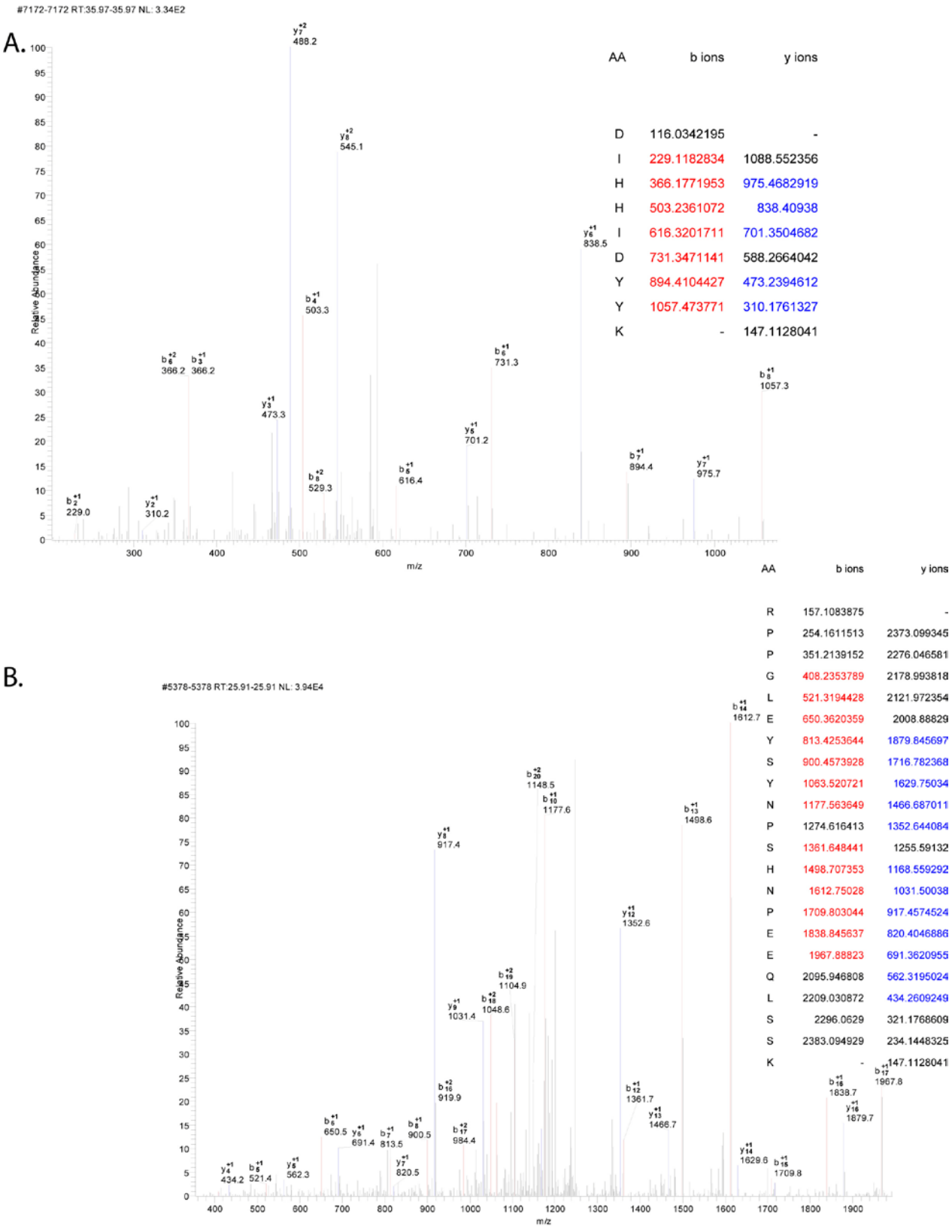
A.
#7172-7172 RT:35.97-35.97 NL: 3.34E2
Relative Abundance
m/z
AA b ions y ions
D 116.0342195 -
I 229.1182834 1088.552356
H 366.1771953 975.4682919
H 503.2361072 838.40938
I 616.3201711 701.3504682
D 731.3471141 588.2664042
Y 894.4104427 473.2394612
Y 1057.473771 310.1761327
K - 147.1128041
B.
#5378-5378 RT:25.91-25.91 NL: 3.94E4
Relative Abundance
m/z
AA b ions y ions
R 157.1083875 -
P 254.1611513 2373.099345
P 351.2139152 2276.046581
G 408.2353789 2178.993818
L 521.3194428 2121.972354
E 650.3620359 2008.88829
Y 813.4253644 1879.845697
S 900.4573928 1716.782368
Y 1063.520721 1629.75034
N 1177.563649 1466.687011
P 1274.616413 1352.644084
S 1361.648441 1255.59132
H 1498.707353 1168.559292
N 1612.75028 1031.50038
P 1709.803044 917.4574524
E 1838.845637 820.4046886
E 1967.88823 691.3620955
Q 2095.946808 562.3195024
L 2209.030872 434.2609249
S 2296.0629 321.1768609
S 2383.094929 234.1448325
K - 147.1128041

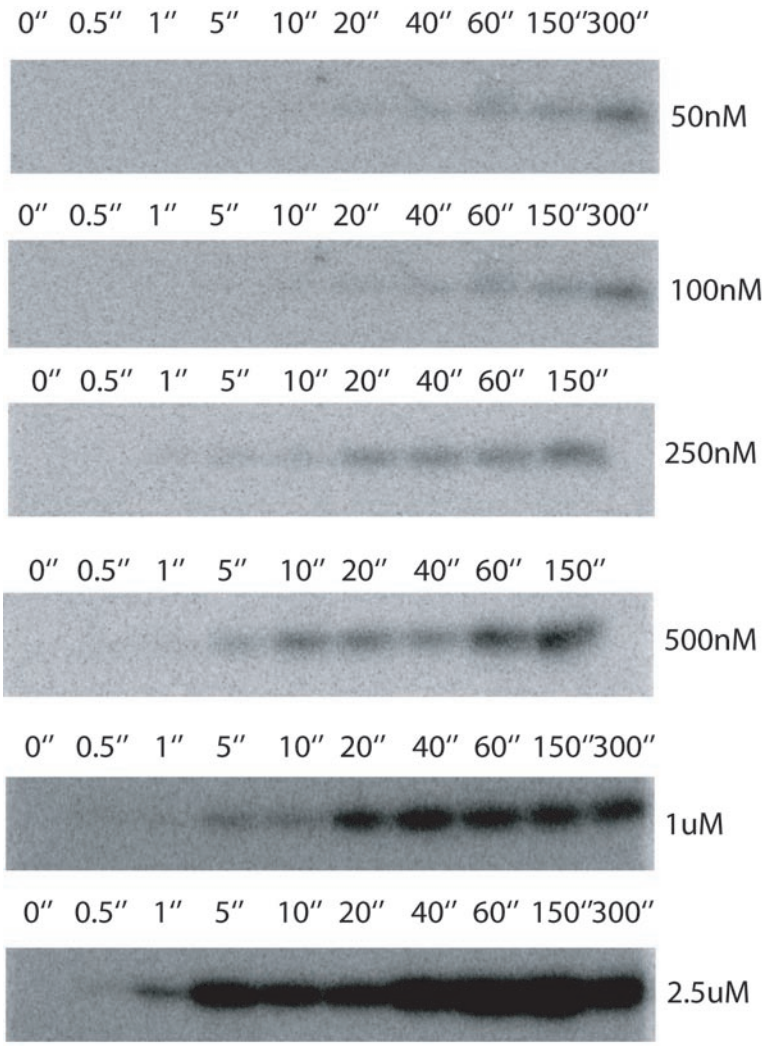

Figure S3. Determination of K_M for FGFR1-mediated Substrate Phosphorylation.

Phosphorylation of kinase-dead substrate (Y^{585}KD) by fully activated kinase. FGFR1-3F-2P kinase (3 μM) was incubated with 50 nM-2.5 μM Y^{583}KD substrate in the presence of 1 mM [γ-^{32}P]-ATP and 2 mM $MgCl_2$ in 10 mM HEPES, pH 7.4 in a rapid chemical quench apparatus at 25^{o}C. The reaction was quenched at various times as indicated upon the addition of 83 mM EDTA, and the formation of the monophosphorylated species over time was followed by incorporation of radiolabeled phosphate. Reactions utilizing concentrations of substrate below 50 nM were below the limit of detection and could not be visualized on the gel.

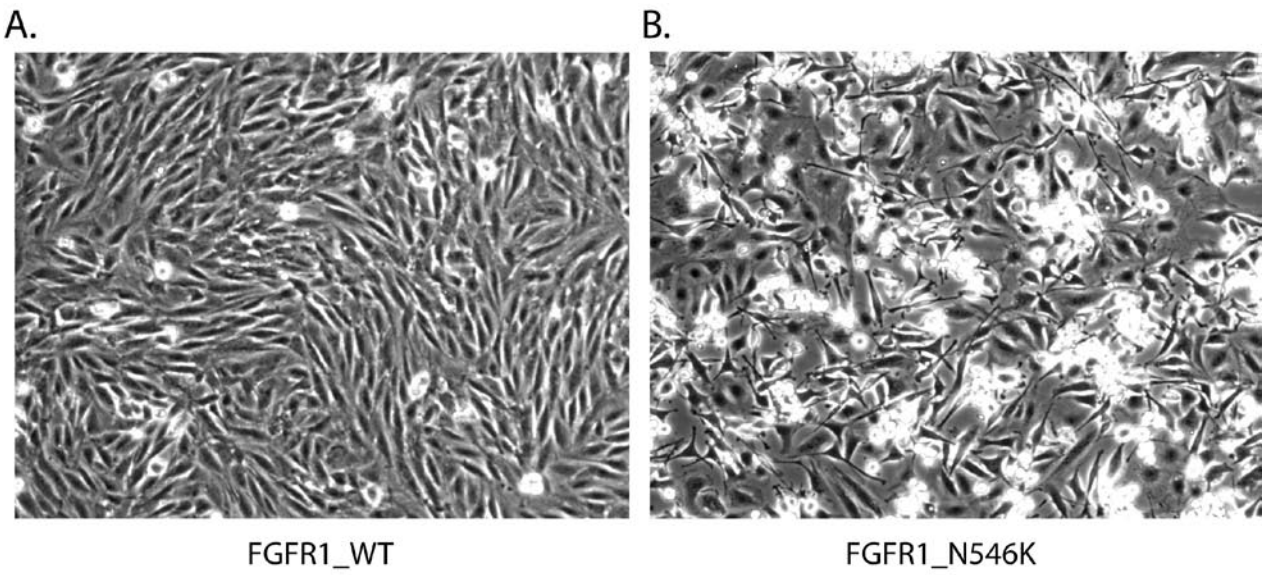

Figure S4. 3T3 Cells Stably Expressing Wild-Type or Mutant FGFR1. 3T3 cells stably expressing either (A) a wild-type FGFR1 or (B) a glioblastoma-derived FGFR1_N546K mutant.

Reaction steps	FGFR1K KinTekSim Mechanism Monophasic	FGFR1K_N546K KinTekSim Mechanism Monophasic	FGFR1K_N546K KinTekSim Mechanism Biphasic
Dimerization $mM^{-1}s^{-1}$	400	400	NA
ATP binding $mM^{-1}s^{-1}$	0.0175	0.0175	NA
$0P \rightarrow 1P, s^{-1}$	0.009	0.09	FP 0.25 SP 0.025
$1P \rightarrow 2P, s^{-1}$	0.008	0.05	FP 0.045 SP 0.009
$2P \rightarrow 3P, s^{-1}$	0.007	0.04	FP 0.015 SP 0.004
$3P \rightarrow 4P, s^{-1}$	0.004	ND	ND
$4P \rightarrow 5P, s^{-1}$	0.003	ND	ND
$5P \rightarrow 6P, s^{-1}$	-	-	-

Table S1. Comparison of Autophosphorylation Kinetics of FGFR1 Kinase (WT) and FGFR1 Kinase Mutant Implicated in Glioblastoma, N546K. Abbreviations: NA: not applicable, FGFR1K dimerization and ATP binding were not included in the biphasic mechanism used for kinetic simulation; FP: fast phase in the biphasic mechanism; SP: slow phase in the biphasic mechanism; ND: not determined, the additional kinetic steps required to describe the biphasic behavior limited the number of phosphorylation events used for kinetic simulation